Bioorganic & Medicinal Chemistry 19 (2011) 5520–5528

Contents lists available at SciVerse ScienceDirect

Bioorganic & Medicinal Chemistry

journal homepage: www.elsevier.com/locate/bmc

Synthesis and photobiological study of a novel chlorin photosensitizer BCPD-18MA for photodynamic therapy

Jialiang Zhang [a,b,†], Li Deng [a,†], Jianzhong Yao [a,*,†], Peng Gu [a], Feng Yang [a], Xiuxin Wang [a], Wei Liu [a], Yingying Zhang [a], Xingfa Ke [a,b], Xiaolong Jing [a,b], Jianming Chen [a,*]

[a] School of Pharmacy, Second Military Medical University, Shanghai 200433, China
[b] Department of Pharmacy, Fujian University of Traditional Chinese Medicine, Fujian 350108, China

ARTICLE INFO

Article history:
Received 23 April 2011
Revised 21 July 2011
Accepted 22 July 2011
Available online 28 July 2011

Keywords:
Cancer
Photodynamic therapy
Liposome
Chlorin
Photosensitizer
Apoptosis
Synthesis

ABSTRACT

This paper reports synthesis and photobiological properties of a novel chlorin photosensitizer BCPD-18MA. Cytotoxicity, cellular uptake, subcellular location, biodistribution, photodynamic therapy (PDT) efficiency, cell apoptosis as well as histological analysis of the liposomal-delivered BCPD-18MA (L-BCPD-18MA) was studied using mammary adenocarcinoma MDA-MB-231 cells and Lewis lung carcinoma (LLC) implanted in C57BL/6 mice as experimental models. The results showed that L-BCPD-18 was incorporated rapidly into MDA-MB-231 cells and localized partially in mitochondria. L-BCPD-18 induced cell apoptosis by PDT. In addition, biodistribution of L-BCPD-18MA in LLC-bearing mice demonstrated a fast clearance rate of the drug and good skin-related tumor selectivity. Finally, entrapment of BCPD-18 into liposomes resulted in a dramatic impairment of dark toxicity and a notable improvement of PDT antitumor efficacy in vitro. Compared with liposomal-delivered BPDMA (L-BPDMA), L-BCPD-18MA exhibited low dark toxicity and high PDT efficiency on MDA-MB-231 cells. The photodynamic efficacy of L-BCPD-18MA on LLC-bearing mice is comparable to that of L-BPDMA, implying that L-BCPD-18MA is a potential antitumor candidate for PDT.

1. Introduction

Photodynamic therapy (PDT) is an attractive alternative in cancer treatment involving combined use of visible light and a photosensitizer (PS).[1–3] Both components of PDT are intrinsically harmless. But after combination with oxygen they can generate cytotoxic reactive oxygen species (ROS) to damage intracellular organelles resulting in cell death.[4,5] Compared with traditional cancer therapies such as surgery, radiotherapy or chemotherapy, PDT offers the opportunity to destroy tumor cells effectively and selectively without causing damage to surrounding healthy tissue.

Porphyrin-type PS such as Photofrin® is the first clinically approved PS for the treatment of bladder cancer in the world.[6] Although there is general agreement that Photofrin® is both efficacious and safe as a treatment for a number of cancer indications,[7–10] it also suffers some drawbacks such as limited selectivity of tumor targeting, cutaneous photosensitivity caused by prolonged persistence of PS in the skin, chemical heterogeneity and inefficient absorption (ε = 1170 M^{-1} cm^{-1}) at long wavelength (λ_{max} = 630 nm).

Compared with porphyrins, chlorin-type PSs are receiving considerable attention owing to their photophysical properties.[6,11] However, many of the compounds developed as potent PSs have limited water hydrophobic solubility, and typically exhibit a better tumor targeting and substantially greater PDT efficacy.[12,13] Due to the obvious limitation of water-insoluble PSs, a vehicle is often needed to deliver the drug to the tumor tissue. Liposomes with a high loading capacity and flexibility to accommodate PSs with variable physicochemical properties come into focus as a valuable carrier and delivery system for hydrophobic PSs. Several studies[14,15] demonstrated that liposomes have significantly high and fast accumulation in tumor tissue as compared with classical drug formulations. As a result, benzoporphyrin derivative monoacid ring A (BPDMA, Fig. 1) with liposomal encapsulation (Visudyne®) is the first clinically approved chlorin-type PS for the treatment of age-related macular degeneration (AMD) in the world.

We previously synthesized a series of novel chlorin-type BPDMA analogues, so-called benzochloroporphyrin derivatives (BCPDs) with hydrophobic features and evaluated their preliminary PDT effects on human heptoma BEL-7402 cells in vitro.[16] Of them, BCPD-18 was of the most potent compounds and relatively convenient to be synthesized. In this study, we further hydrolyzed BCPD-18 to form a monoacid derivative BCPD-18MA (Fig. 1) with the aim to improve its tumoritropic behavior and hydrophilicity, and used liposome as a carrier and delivery system to prepare liposomal-delivered BCPD-18MA (L-BCPD-18MA) in an attempt to investigate its photophysical properties, cellular uptake, dark toxicity, PDT

* Corresponding authors. Tel./fax: +86 21 81871235 (J.Y.); +86 21 81871291 (J.C.).
E-mail addresses: yaojz@sh163.net (J. Yao), yjcjm@163.com (J. Chen).
† These authors contributed equally to this work.

0968-0896/$ - see front matter © 2011 Elsevier Ltd. All rights reserved.
doi:10.1016/j.bmc.2011.07.041

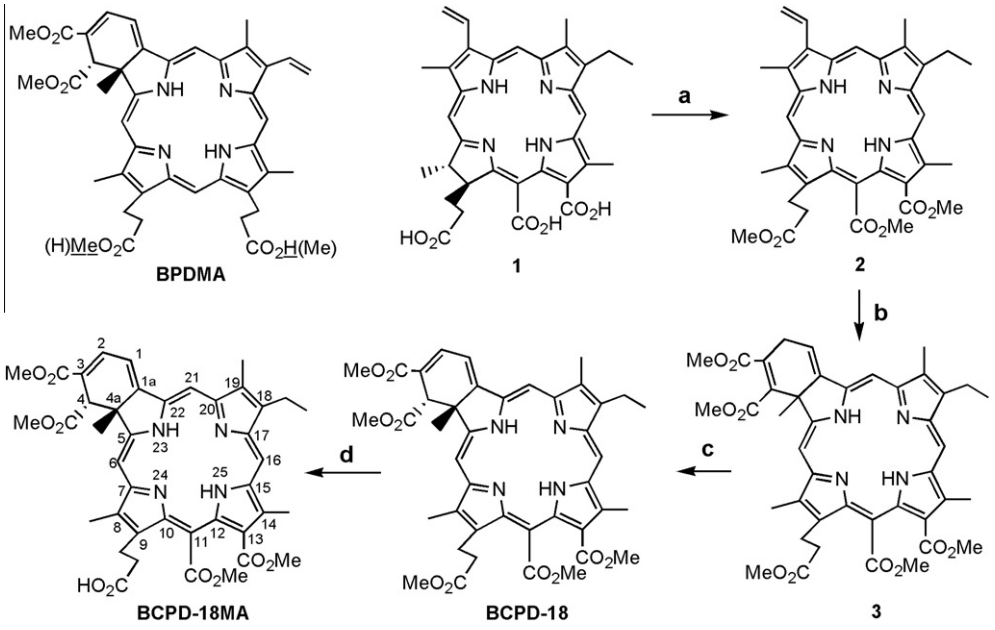

Figure 1. Structure of BPDMA and synthetic scheme of BCPD-18MA. Reaction conditions: (a) (1) CH_2N_2, Et_2O, 0 °C, 10 min, (2) DDQ, CH_2Cl_2–benzene (5:1), rt, 30 min; two step 52.9%, (b) DMAD, toluene, reflux, 6 d, 43.4%, (c) DBU, CH_2Cl_2, rt, 30 min, 94.7%, (d) THF–25% aqueous HCl (1:1), rt, 2.5 h, 96.8%.

efficiency in vitro, subcellular location, cell apoptosis, biodistribution and PDT anticancer efficacy in vivo, in addition to histological analysis using mammary adenocarcinoma MDA-MB-231 cells and Lewis lung carcinoma (LLC) subcutaneously implanted in C57BL/6 mice as experimental models.

2. Results and discussion

2.1. Chemical synthesis

The novel chlorin-type photosensitizer BCPD-18MA was prepared in multistep synthetic sequence (Fig. 1). The synthetic sequence started with chlorin p_6 **1**, a degradation product of the easily accessible crude chlorophyll extract from a Chinese traditional herb silkworm excrement.[17] The methylation of **1** with CH_2N_2 followed by oxidation with 2,3-dichloro-5,6-dicyano-1, 4-benzoquinone (DDQ) afforded chloroporphyrin p_6 trimethyl ester **2**. Upon treatment of **2** with dimethyl acetylenedicarboxylate (DMAD) in refluxing toluene provided the Diels–Alder adducts **3**. Rearrangement of **3** with 1,8-diazabicyclo[5,4,0]undec-7-ene (DBU) gave the conjugated BCPD-18 with a 94.7% yield.[16] BCPD-18 was transformed into its monoacid derivative BCPD-18MA with a 96.8% yield by selective hydrolyzation with aqueous 18% HCl. The structure of BCPD-18MA was confirmed by ^{1}H NMR, HRMS spectroscopy and elemental analysis, and its UV–vis spectrum in $CHCl_3$ showed the strongest long wavelength absorption at 678 nm ($\varepsilon = 2.36 \times 10^4\ M^{-1}\ cm^{-1}$).

2.2. Photophysical study

As shown in Figure 2, the concentration of BCPD-18MA was reduced about 12% after 10 min exposure to light (300 mW/cm^2, 180 J/cm^2) and the photo-degradation process was not accompanied by the appearance of new absorption bands in the visible wavelength range, indicating that no photoproduct that could potentially bring about further photosensitising activity was formed, which is contrary to what was previously reported for other porphyrins such as protoporphyrin IX.[18] In addition, these findings also imply that illumination (300 mW/cm^2, 150 J/cm^2) only destroyed small amounts of the PS, and that the PDT conditions used in our in vivo study should be rational.

2.3. Biological study

2.3.1. Cellular uptake of BCPD-18MA

BCPD-18MA uptake in MDA-MB-231 cells was evaluated using a concentration of 2 μg/ml at different incubation times. In each case, the PS intracellular concentration was determined by fluorescence analysis. As shown in Figure 3, L-BCPD-18MA was rapidly incorporated into MDA-MB-231 cells in the initial time (<4 h)

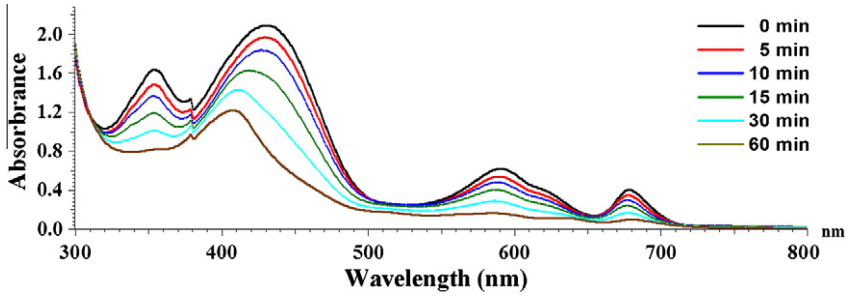

Figure 2. Visible absorption spectra of BCPD-18MA (15 μg/ml, 300 mW/cm^2) at different irradiation times.

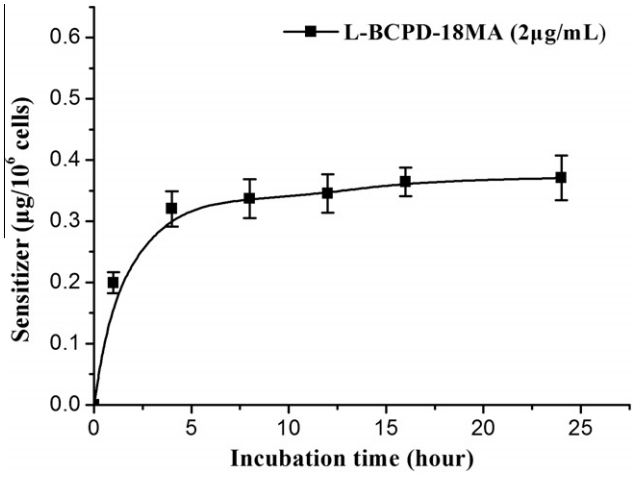

Figure 3. BCPD-18MA uptake in MDA-MB-231 cells via liposomal vehicles as a function of incubation time. Data represent the mean ± SD, $n = 3$.

and its cellular uptake reached a saturation value between 4 and 24 h. This value was estimated as ~0.35 μg /10^6 cells.

2.3.2. Dark toxicity and PDT efficiency of BCPD-18MA

Dark toxicity and PDT efficiency of BCPD-18MA in MDA-MB-231cells via the liposomal vehicle (L-BCPD-18MA) or after being dissolved in dimethyl sulfoxide followed by dilution with Dulbecco's modified Eagle's medium (F-BCPD-18MA) were compared with L-BPDMA as the positive control (Fig. 4).

Figure 4A shows that L-BCPD-18MA exhibited lower dark toxicity than either L-BPDMA or F-BCPD-18MA after 24 h incubation with MDA-MB-231cells in a dose-dependent manner. When the concentration was less than 6 μM, L-BCPD-18MA did not lead to any significant decrease in survival fraction.

As shown in Figure 4B, cell survival fraction decreased when the PS concentration and the light dose were raised. No cytotoxicity was induced upon exposure of MDA-MB-231 cells to light alone. Meanwhile, it was found that cell survival fraction for L-BCPD-18MA was significantly lower than that for either L-BPDMA or F-BCPD-18MA in the same conditions, indicating that L-BCPD-18MA had greater PDT efficiency than either L-BPDMA or F-BCPD-18MA against MDA-MB-231cells in a dose-dependent manner, and cell death was only triggered by a combination of the PS and light.

All these results showed that both PDT efficiency and dark toxicity were improved by liposomalization. The improvement of the photocytotoxic efficiency of BCPD-18MA-mediated PDT by its encapsulation into small sized liposomes may be due to effective drug delivery to tumor cells. Indeed, it is reported[19] that submicron-sized liposomes have relatively higher intracellular uptake compared with aqueous solution.

2.3.3. Subcellular location of BCPD-18MA

The location of the PS is of special significance, since it determines the site of primary photodamages and the type of cellular response to the therapy. While singlet oxygen ($^1O_2$) has a very short lifetime in cells, its intracellular targets are close to the sites where the PS is located. Therefore, cellular structures containing PS would be preferentially damaged upon illumination.

The preferential sites of subcellular localization of BCPD-18MA were evaluated by Laser confocal microscopy upon exposure of MDA-MB-231 cells to L-BCPD-18MA (1 μg/ml) for 24 h. Figure 5 shows the fluorescent pattern observed for BCPD-18MA and its overlay with the organelle specific fluorescent probes LysoTracker Green® (lysosomes) and MitoTracker® Green FM (mitochondria). The images were obtained by merging the fluorescence of LysoTracker Green® DND-26 (green signal, Fig. 5C) or MitoTracker® Green FM (green signal, Fig. 5G) with that of BCPD-18MA (red signal, Fig. 5B and F). After entry into cells, BCPD-18MA was found to localize in the cytoplasm around the nucleus of MDA-MB-231 cells. No accumulation of BCPD-18MA was observed inside the nucleus. The restriction of PS from the nucleus may minimize the mutagenic potential of cells given sublethal intensities of PDT.[20] The merged stained images revealed a partial overlap of BCPD-18MA and MitoTracker® Green FM (yellow signal), suggesting that mitochondria were the site of intracellular distribution of BCPD-18MA (Fig. 5H). Mitochondria are very important cell organs related to apoptosis, which is of special significance in cancer treatment.[21] For lysosomes, the merged stained images revealed no overlap of BCPD-18MA and LysoTracker Green® signals, indicating that lysosomes were not sites of intracellular distribution of BCPD-18MA (Fig. 5D).

2.3.4. Detection of apoptotic cells

Many PSs can induce apoptosis of malignant cells.[22–24] Apoptosis is of special importance in cancer treatment. To see whether BCPD-18MA could induce cell apoptosis, two aspects of apoptosis were studied: nuclear fragmentation and phosphatidylserine exposure.

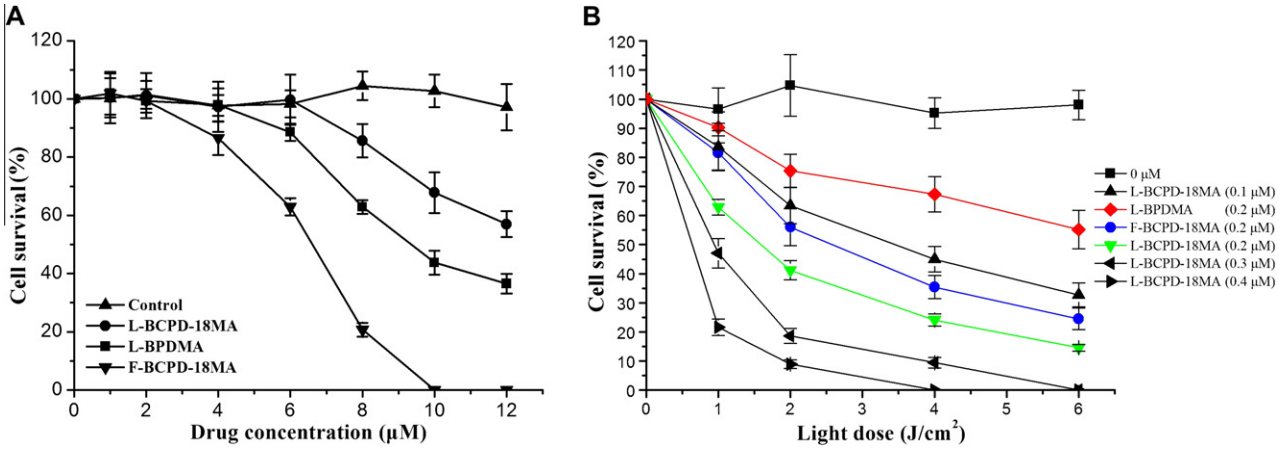

Figure 4. Effects of BCPD-18MA cytotoxicity on MDA-MB-231 cells. Data represent the mean ± SD, $n = 6$. (A) Dark toxicity after incubation for 24 h with photosensitizers without irradiation. (B) Phototoxicity after incubation for 4 h with photosensitizers and then irradiation with various light doses.

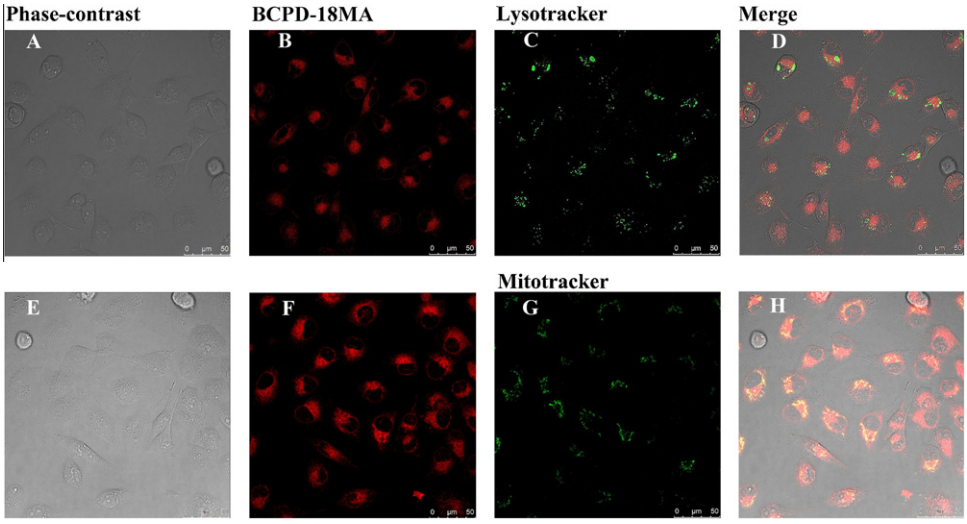

Figure 5. Intracellular location of 1 μg/ml BCPD-18MA in MDA-MB-231 cells after 24 h incubation. MDA-MB-231 cells were incubated with both BCPD-18MA and LysoTracker® Green DND-26 (100 nM, for 60 min) or MitoTracker® Green FM (100 nM, for 30 min). Red fluorescence corresponds to BCPD-18MA (B or F) while green fluorescence represents the signal from Lyso Tracker Green DND-26 (C) or MitoTracker® Green FM (G). The merged stained image reveals no overlap of BCPD-18MA and LysoTracker Green® signal (D). Yellow fluorescence indicates regions of BCPD-18MA and MitoTracker® Green FM signal overlap (H). Images are representative of those obtained in three independent experiments. Scale bar: 50 μm.

Analyses of nuclear morphology by DAPI staining are shown in Figure 6A. Photographic characteristics of normal cells are indicated in Figure 6Aa. Death of apoptotic cells was identified not only by the occurrence of cell rounding, shrinkage and deformation but also by the typical nuclear fragmentation (Fig. 6Ab).

The redistribution of plasma membrane phosphatidylserine is an early marker of apoptosis. Since Annexin V-FITC can also be used to detect necrotic cells as a result of the loss of membrane integrity, apoptotic cells were differentiated from necrotic cells by an increase in PI positivity, which selectively labels necrotic but not apoptotic cells. To monitor the concentration gradient of phosphatidylserine exposure, Annexin V-FITC binding and PI uptake were measured by flow cytometry. The percentage of cells displaying phosphatidylserine exposure suggestive of apoptosis is shown in Figure 6B. An increase in phosphatidylserine translocation was observed at 4 h post-irradiation at a dose of 0.5 μg/ml (Fig. 6Bb) or 1 μg/ml (Fig. 6Bc). Looking at Figure 6Bb or Bc, while there was an increase in the population of apoptotic cells (lower right quadrant), it was obvious that there was an even more significant increase in the population of necrotic cells (upper right). It was because lower right quadrant only represented early period apoptosis cells, and upper right quadrant represented not only necrotic cells but also late period apoptosis cells. Moreover, due to upper left quadrant representing cell fragment produced by L-BCPD-18MA-mediated PDT, the presence and increase in cell fragment population at the upper left quadrant indicated that the L-BCPD-18MA-mediated PDT could damage the target cells.

Our previous studies[16] demonstrated that BCPD-16 (an analogue of BCPD-18MA) could induce cell apoptosis for PDT treatment. Both nuclear fragmentation and phosphatidylserine exposure are criteria for apoptosis.[25,26] Flow cytometry in our study observed typical nuclear fragmentation in nuclear morphology and phosphatidylserine exposure after BCPD-18MA-mediated PDT, indicating that BCPD-18MA-mediated PDT also could induce cell apoptosis (Fig. 6), supporting that BCPD-18MA-treated cells underwent apoptosis.

2.3.5. BCPD-18MA biodistribution

An ideal PS should accumulate specifically in the tumor and can be cleared away from other tissues rapidly. In our study on BCPD-18MA biodistribution, L-BCPD-18MA was administered intravenously in LLC-bearing mice at a dose of 4 mg/kg body weight, and the amount of PS present in the tissue or plasma was quantified by fluorescence spectroscopy.

As shown in Figure 7A, the biodistribution of L-BCPD-18MA was not uniform. The maximum concentration of BCPD-18MA in healthy tissues of inner organs was observed at 15 min after L-BCPD-18MA administration. The largest accumulation of L-BCPD-18MA was found to occur in the liver. This observation is in agreement with the known tendency of most PSs in clinical use. Excretion was from the liver into the bile and then to the intestine, where it was excreted via fecal elimination.[27] Low amounts of L-BCPD-18MA (<2000 ng/g) were found in other tissues and organs, including the heart, spleen, kidneys and lungs. After 5 h post injection, the drug concentration in the heart, spleen and kidneys was around the detection limit (50 ng/g), and could not be detected in the lungs. The drug could be detected only in the liver at 12 h after drug administration (Data not shown), indicating that the drug could be cleared away from the normal tissues rapidly.

As shown in Figure 7B, there was no significant fluctuation in the drug concentration accumulated in either the tumor or the skin surrounding the tumor within 5 h. Compared with the skin, a relatively great amount of the drug was accumulated in the tumor. The maximum concentration of the drug in the tumor occurred at 1 h after L-BCPD-18MA administration, while the maximum ratio (3.79) of the drug concentration in the tumor and in the skin around the tumor was observed at 3 h post drug injection. The optimal treatment time for PDT seemed to be at 3 h post injection, which is similar to that of L-BPDMA,[28] knowing that PDT has a relatively stronger tumor inhibition and weaker damage to the skin around the tumor at this time.

2.3.6. PDT efficacy of BCPD-18MA on LLC-bearing mice

PDT antitumor efficacy of BCPD-18MA against LLC implanted in C57BL/6 mice was evaluated by tumor growth-inhibition analysis. The tumor size was measured 30 days after treatment. The results are shown in Figure 8.

As shown in Figure 8, the size of tumors in LLC-bearing mice in the three negative control groups increased during the observation period, though there was no statistically significant difference

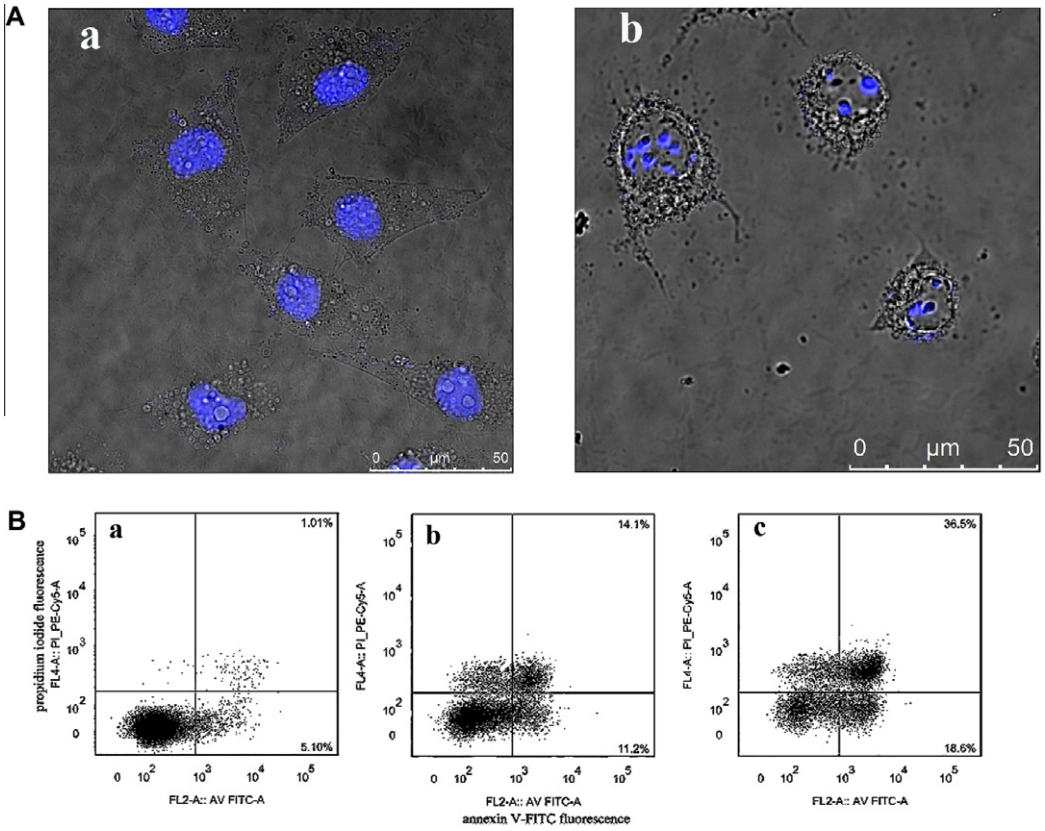

Figure 6. Fluorescence photomicrographs of MDA-MB-231 cells stained with DAPI, representing as overlay of DAPI fluorescence and phase contrast (A): (a) Untreated cells, (b) Cells induced by treatment with L-BCPD-18MA (1 μg/ml) and exposure at a light dose of 10 J/cm^2 at room temperature; Scale bars = 50 μm. Flow cytometry analysis of MDA-MB-231 cells with Annexin V/PI double staining after PDT (B): (a) Control; (b) Treated with 0.5 μg/ml of L-BCPD-18MA at a light dose of 10 J/cm^2; (c) Treated with 1 μg/ml of L-BCPD-18 at a light dose of 10 J/cm^2. UL (upper left quadrant), Annexin V (−) PI (+), cell fragment; UR (upper right quadrant), Annexin V (+) PI (+), necrosis or the late period apoptosis; LL (lower left quadrant), Annexin V (−) PI (−), survival cell; LR (lower right quadrant), Annexin V (+) PI (−), early period apoptosis.

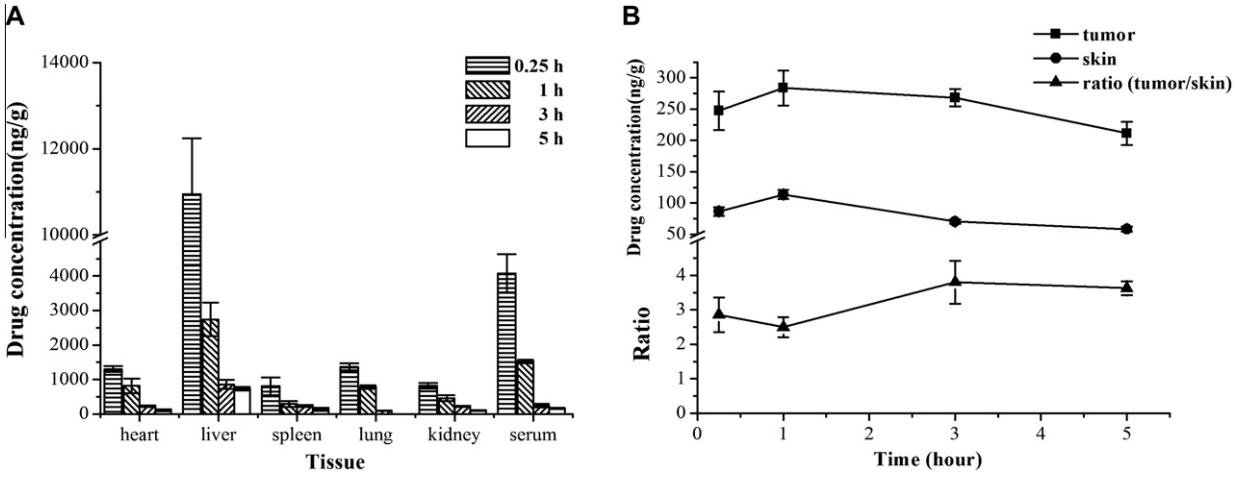

Figure 7. L-BCPD-18MA biodistribution after iv injection (4 mg/kg) in LLC-bearing mice. Concentrations of BCPD-18MA as a function of the tissues and serum at different times (A). Concentrations of BCPD-18MA in tumor and skin as a function of time and concentration ratios of tumor to skin at different times (B). All data represent mean ± SD, $n = 5$.

between the three groups. Compared with the negative control groups, growth of the implanted tumors in the three L-BCPD-18MA-PDT groups and L-BPDMA-PDT group (positive control) was inhibited significantly, as represented by reduced tumor volumes. There was statistically significant difference in tumor volume between the treatment groups and the negative control groups throughout the observation period (P <0.05 or <0.01), while there was no significant difference in tumor volume between L-BPDMA-PDT (0.5 mg/kg) and L-BCPD-18MA-PDT (0.5 mg/kg) groups (P >0.05), suggesting that L-BCPD-18MA possessed the same photodynamic antitumor efficacy on LLC-bearing mice as L-BPDMA.

On the other hand, tumor growth was almost completely inhibited for two weeks in L-BCPD-18MA-PDT group (1 mg/kg), while tumor growth was delayed for only 5–6 days in either L-BPDMA-PDT (0.5 mg/kg) or L-BCPD-18MA-PDT (0.5 mg/kg) group. In

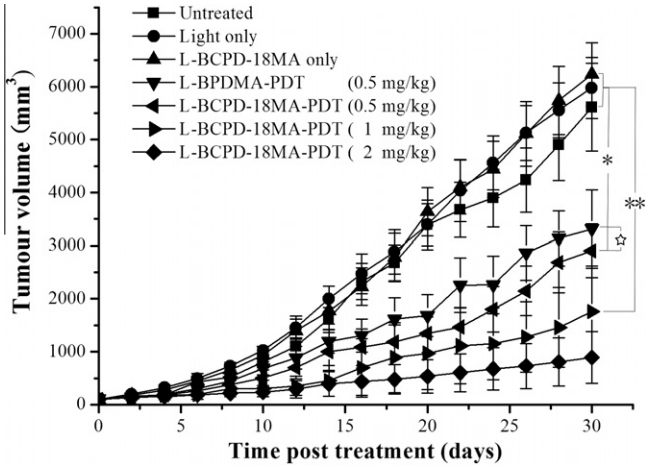

Figure 8. PDT efficacy on LLC-bearing mice. Tumors were either untreated or treated with light only, L-BCPD-18MA (2 mg/kg) only, L-BCPD-18MA-PDT (0.5 mg/kg and light exposure), L-BCPD-18MA-PDT (1 mg/kg and light exposure), L-BCPD-18MA-PDT (2 mg/kg and light exposure), L-BPDMA-PDT (0.5 mg/kg and light exposure). The data represent the mean ± SD of the volumes of 10 tumors in each group. Dosage of light: 150 J/cm^2. $^*P$ <0.05, $^{**}P$ <0.01; $^{\star}P$ >0.05.

addition, tumors in 1 mg/kg and 2 mg/kg L-BCPD-18MA-PDT groups were swollen and hyperemic, provoking an inflammatory reaction at the PDT-treated site, as evidenced by the appearance of typical signs of inflammation as reported by Dougherty et al.[12] The PDT antitumor efficacy of L-BCPD-18MA exhibited an obvious dose-effect relationship.

It was reported that liposomal delivery of PSs could improve the selectivity of drug accumulation in cancer cells[29–32] and strongly increase photodynamic efficiency of PSs.[30,32] Liposomal formulation was found to improve the tumor uptake of PS via LDL-receptor-mediated endocytosis[33,34] because tumor cells were reported to express an elevated number of LDL-receptors due to their rapid proliferation and increased cholesterol demand for membrane synthesis.[33,35] A number of reports comparing the PDT outcome of liposomal versus non-liposomal PSs provided strong evidence that liposomal formulation could be advantageous under identical conditions.[33]

2.3.7. Histological analysis

One ideal PS should not be toxic per se without irradiation in the concentration range applied in PDT and could cause great damage to the tumor after PDT treatment.

No general features of cardiac, hepatic, splenic, pneumal and renal injury were observed in our histological study with microscopic images of the H&E-stained heart, liver, spleen, lung and kidney sections obtained from LLC-bearing mice in L-BCPD-18MA-treated (5 mg/kg without light exposure) group (Fig. 9Aa–e), suggesting that BCPD-18MA per se did not induce any significant damage to normal organs.

Microscopic histology images of the tumor tissue taken from LLC-bearing mice in control group showed evidence of typical malignancy (Fig. 9Ba). On the contrary, tumor histological images from L-BCPD-18MA-treated LLC-bearing mice receiving light illumination (150 J/cm^2) after drug administration at dosage of 0.5, 1 and 2 mg/kg showed poorly active tumoral masses and cell necrosis in varying degrees, indicating that BCPD-18MA could significantly damage the tumor after PDT treatment (Fig. 9Bb–d).

3. Conclusions

We have for the first time rationally designed and successfully synthesized a novel chlorin-type photosensitizer BCPD-18MA as a BPDMA analogue, and prepared liposomal-delivered BCPD-18MA (L-BCPD-18MA). Our cellular uptake study showed that L-BCPD-18MA could rapidly incorporate into MDA-MB-231 cells within 4 h. When loaded into MDA-MB-231 cells, BCPD-18 was localized mainly within the cytoplasmic region and partially in mitochondria. Analyses of phosphatidylserine exposure and nuclear fragmentation indicate that BCPD-18MA-mediated PDT could induce cell apoptosis. Biodistribution study of L-BCPD-18MA in LLC-bearing mice confirmed its fast rate of clearance and good tumor selectivity related to the skin. Compared with F-BCPD-18MA, entrapment of BCPD-18MA into liposomes resulted in a dramatic impairment of dark toxicity and a notable improvement of PDT antitumor efficiency against MDA-MB-231 cells. In addition, relative to L-BPDMA, L-BCPD-18MA exhibited lower dark toxicity and higher phototoxicity against MDA-MB-231 cells and the equal photodynamic efficacy on LLC implanted in C57BL/6 mice receiving light treatment after 3-h iv injection. HE-stain investigations of inner organs and tumor specimens showed that BCPD-18MA-mediated PDT could cause serious damage to the tumor, and BCPD-18MA per se did not induce any significant injury to normal organs.

In summary, our data support the idea that L-BCPD-18MA is a valuable antitumor candidate for further preclinical PDT development due to its strong absorption at 678 nm ($\varepsilon = 2.36 \times 10^4$ M^{-1} cm^{-1}), rapid clearance from tissues, good skin-related tumor selectivity, low dark toxicity and high photocytotoxicity on

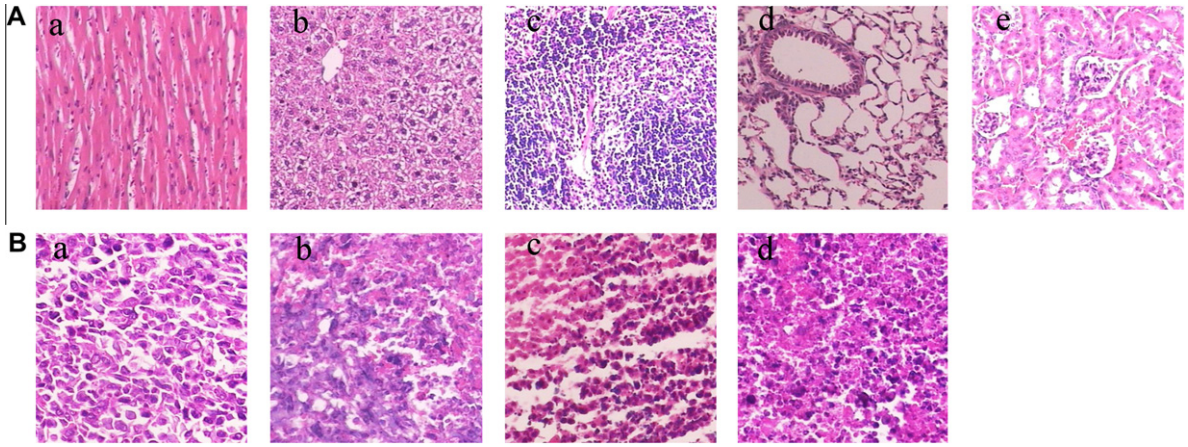

Figure 9. Microscopic images obtained after H&E staining of the heart, liver, spleen, lung and kidney sections from L-BCPD-18MA-treated LLC-bearing mice (5 mg/kg, without light irradiation) (Aa–e). Nuclei were stained by haematoxylin solution (purple) and the cytoplasm was counterstained by eosin solution (pink) (×200). Microscopic appearance of the tumor specimen obtained from control group LLC-bearing mice stained by H&E, showing typical evidence of malignancy (Ba) (×200). H&E staining micrographs of the tumor tissue obtained from L-BCPD-18MA-PDT LLC-bearing mice after administration at the drug dosage of 0.5, 1 and 2 mg/kg body weight and a light dose of 150 J/cm^2, showing poorly active tumoral mass and cell necrosis in varying degrees (Bb–d) (×200).

MDA-MB-231 cells, as compared with either F-BCPD-18MA or L-BPDMA. The photodynamic efficacy of L-BCPD-18MA on LLC-bearing mice is comparable to that of L-BPDMA.

4. Experimental section

4.1. (±)-Trans-3,4-dimethoxycarbonyl-4,4a-dihydro-4a,8,14,19-tetramethyl-18-ethyl-23*H*,25*H*-benzo[*b*] porphine-11,13-dimethoxycarbonyl-9-propanoic acid (BCPD-18MA)

BCPD-18 was synthesized as described by Yao et al.[16] The foregoing BCPD-18 (40 mg, 0.052 mmol) was dissolved in THF (10 ml) with addition of 25% HCl aqueous solution (10 ml). The reaction mixture was stirred at room temperature for 2.5 h. After evaporation of the solvent, the residue was purified on silica gel column, eluting with CH_2Cl_2/MeOH (10:0.25, v/v). The dark green eluate was collected and concentrated to give BCPD-18MA as a black powder. Yield: 38 mg (96.8%). Mp 190–191 °C. UV–vis λ_{max} ($CHCl_3$, nm): 441 (soret band, 1.09×10^5), 590 (3.07×10^4), 678 (2.36×10^4). ^{1}H NMR (DMSO, δ, ppm): 12.43 (s, 1H, CO_2H), 9.88, 9.68 and 9.41 (each s, each 1H, 6-, 16- and 21-H), 7.83 (d, 1H, J = 5.6 Hz, 2-H), 7.78 (d, 1H, J = 5.6 Hz, 1-H), 5.34 (s, 1H, 4-H), 4.25, 4.15, 3.93, 3.49, 3.47, 3.45 and 2.96 (each s, each 3H, 4 × OMe and 8-, 14-,19-Me), 3.97 (m, 2H, J = 7.5 Hz, 18^1-CH_2), 3.81 (m, 2H, J = 8.4 Hz, 9^1-CH_2), 2.90 (m, 2H, J = 8.4 Hz, 9^2-CH_2), 1.79 (s, 3H, 4a-Me), 1.71 (t, 3H, J = 7.5 Hz, 18^2-Me), −2.08 and −2.39 (each s, each 1H, NH × 2). HRMS (m/z) calcd for $C_{41}H_{42}N_4O_{10}$: 750.2894; found: 750.2901. Elemental Anal. Calcd for $C_{41}H_{42}N_4O_{10}\cdot H_2O$: C, 64.06; H, 5.72; N, 7.29. Found: C, 63.92; H, 5.70; N, 7.32. HPLC: Agilent RP18; MeOH/THF/H_2O/HOAc (57:32:10:1, volume ratio); t_R = 3.64 min; relative purity: 98.91%.

4.2. Photophysical study

4.2.1. Preparation of L-BCPD-18MA, L-BPDMA and F-BCPD-18MA

L-BCPD-18MA and L-BPDMA were prepared according to the method of Bangham et al.[36] with minor modifications. 1,2-dimyristoyl-sn-glycero-3-phosphocholine (DMPC, lipoid, Germany), egg phosphatidyl glycerol (EPG, lipoid, Germany) and BCPD-18MA or BPDMA (United States Pharmacopeia, Maryland, America) (7:3:1, molar ratio) dissolved in dichloromethane were evaporated to form a thin lipid film under reduced pressure, and stored in vacuo with a water bath at 40 °C for at least 1 h. The thin lipid film was then hydrated with phosphate buffered saline (PBS, pH 7.4, Hyclone Thermo Scientific, Beijing, China). The liposome suspension was extruded twice through a polycarbonate membrane filter with 0.2 μm pores, and then passed through a polycarbonate membrane filter with 0.08 μm pores twice to obtain size-homogeneous liposomes. Suspension of the resulting liposomes was extruded through sterile Millipore Express with 0.22 μm pore size to remove the bacteria. The preparation was used within a week.

F-BCPD-18MA was prepared by dissolving BCPD-18MA in dimethyl sulfoxide (DMSO) followed by dilution with Dulbecco's modified Eagle's medium (DMEM) (the volume content of DMSO in F-BCPD-18MA solution was less than 0.02%).

4.2.2. Photo-degradation study of BCPD-18MA

L-BCPD-18MA was placed in a quartz cuvette of 1 cm optical path and gently stirred during irradiation, which was performed by using red light at 678 ± 2 nm. The rate of BCPD-18MA photodegradation was determined spectrophotometrically by measuring the variations in the absorption spectrum in the 300–800 nm wavelength interval upon exposure of L-BCPD-18MA (15 μg/ml) in aqueous dispersions of liposomal vesicles to the diode laser (bandwidth 678 ± 2 nm, power range 0–1 W, nLIGHT, Hillsboro, America), which was operated at a fluence rate of 300 mW/cm^2.

4.3. Biological study

4.3.1. Cell lines and cell culture

Human mammary adenocarcinoma MDA-MB-231 and mice Lewis lung carcinoma (LLC) cells were originally obtained from the Chinese Academy of Sciences Shanghai Institute of Cell Bank (Shanghai, China). MDA-MB-231 and LLC cells were maintained in DMEM in 5% CO_2, 95% air in a humidified incubator at 37 °C. All the media were supplemented with 10% fetal bovine serum (FBS, Gibco Invitrogen, Victoria, Australia).

4.3.2. The mouse tumor model

C57BL/6 male mice aged 5 weeks with a mean body weight of 16 ± 2 g were purchased from Shanghai SLAC Laboratory Animal Co., Ltd (Shanghai, China). To develop the tumor model, LLC cells (1×10^6) were subcutaneously inoculated into the left posterior flank of the mice. Measurement of the tumor size was started on day 10.

Tumor-bearing mice were used for biodistribution study when the tumor grew to about 1.2–1.5 cm in diameter.

Two parameters (length and width) of the tumor were measured using a micrometer digital caliper (500-157-20, Mitutoyo, Japan) for calculation of the tumor volume. The tumor volume was calculated using the following formula: $V = (W^2 \times L)/2$, according to the US National Cancer Institute protocol, where W is the width and L is the length of the tumor. Only those mice with tumor volume between 75 and 120 mm^3 were used. The animals were given free access to food and water during the experiment.

4.3.3. Cellular uptake of BCPD-18MA

The intracellular concentration of BCPD-18MA was estimated based on the number of cells. MDA-MB-231 cells (1×10^6 cells) were cultured in a 10-cm petri dish and incubated for 24 h. The culture medium DMEM in the petri dish was replaced with a fresh culture medium containing L-BCPD-18MA supplemented with 10% (v/v) FBS. The cells were then incubated with 2 μg/ml of L-BCPD-18MA during a time lapse of 1, 4, 8, 12, 16, 24 h at 37 °C in the dark. After incubation, the cells were washed twice with ice-cold PBS and harvested by scraping the bottom of the dish with 2 ml PBS by using a cell scraper and aspirating vigorously to obtain a single cell suspension. The amount of the viable cells was counted with trypan blue (TB, Sigma Chemical Co., St. Louis, USA) exclusion test using a Neubauer chamber counter. The cell suspension was centrifuged at 1000g/min for 5 min to obtain the cell pellet. The cells pellet was dispersed in 2 ml 3% sodium dodecyl sulphate (SDS, Sigma Chemical Co., St. Louis, USA). The extraction of BCPD-18MA from the cells was facilitated by agitation. The amount of BCPD-18MA was fluorometrically determined with an excitation wavelength of 440 nm and an emission wavelength of 685 nm using a fluorescence spectrophotometer (F7000, Hitachi). Quantification of BCPD-18MA was carried out using calibration curves generated with various known concentrations of BCPD-18MA. The kinetics of uptake (concentration of drug/10^6 cells vs time) was calculated.

4.3.4. Dark toxicity and PDT efficiency of BCPD-18MA

MDA-MB-231 cells were cultured in DMEM medium supplemented with 10% (v/v) FBS, harvested with 0.25% (w/v) trypsin (Gibco Invitrogen, Australia), and seeded in 96-well plates at 5×10^3 cells per well. The cells were allowed to attach to the bottom of the wells for 12 h prior to start of the experiment.

The dark toxicity characteristic of each group was assessed with different concentrations (range from 1 to 12 μM). Cells were exposed to graded doses of L-BCPD-18MA, F-BCPD-18MA and L-BPDMA for 24 h. The surviving fraction of cells was immediately evaluated using the 3-(4,5-dimethylthiazol-2-yl)-2,5-diphenyltetrazolium bromide (MTT, Sigma Chemical Co., St. Louis, USA)

spectrophotometric method. Precautions were taken to avoid exposure of the cells to light throughout the experimental period when the cells were exposed to, or contained PSs.

Phototoxicity of each group was assessed with different light doses (1, 2, 4, 6 J/cm^2) and different concentrations (range from 0 to 0.4 μM) separately following a similar procedure for dark toxicity. After 4 h incubation with L-BCPD-18MA, F-BCPD-18MA or L-BPDMA, the cells were exposed to the light and the light intensity at the treatment site was 5 mW/cm^2. The surviving fraction of cells was evaluated by MTT assay 24 h after treatment.

4.3.5. Subcellular location of BCPD-18MA

MDA-MB-231 cells were cultured in DMEM medium supplemented with 10% FBS. The cells were seeded in thin glass-bottomed 35 mm petri dishes (NEST Biotechnology, Hangzhou, China) at 1×10^4 cells per dish and incubated for 12 h at 37 °C under 5% CO_2 atmosphere to reattach. Freshly prepared solutions of L-BCPD-18MA were diluted with the medium. The medium was removed from the dishes and 2 ml fresh medium containing PS at a concentration of 1 μg/ml was added to the dishes, and the cells were incubated at 37 °C under 5% CO_2 atmosphere in dark for 24 h. The medium was removed and the cells were washed twice with PBS, followed by incubation at 37 °C with LysoTracker® Green DND-26 (100 nM, for 60 min, Molecular Probes, Oregon, USA) or MitoTracker® Green FM (100 nM, for 30 min, Molecular Probes, Oregon, USA). Then, the cells were examined using a Leica TCS SP5 spectral confocal microscope equipped with Argon–HeliumNeon (Ar–HeNe) laser. Mitochondria- and lysosome-specific probes and BCPD-18MA were excited at the wavelength of 496, 505, 440 nm separately. Emission lines were collected after passage through a filter ranging from 510 to 550 nm for MitoTracker® Green FM and LysoTracker® Green DND-26, and from 650 to 700 nm for BCPD-18MA. Signals from different fluorescent probes were acquired in a sequential scan mode, allowing the elimination of channel cross-talk, and co-localization was detected in an overlay mode. Acquisition parameters were as follows: Lens 63x/1.4 Oil; image size: 1024×1024; pinhole size: 1 Airy. Images were processed by using LCS (Leica Microsystems. Heidelberg Gmbh, Germany).

4.3.6. Detection of apoptotic cells following PDT treatment

To assess changes in nuclear morphology typical of apoptosis, MDA-MB-231 cells were incubated with 1 μg/ml L-BCPD-18MA. After 24 h incubation, the drug-containing medium was refreshed, and cells were exposed to the laser (50 mW/cm^2, 10 J/cm^2). After being illustrated, cells were continually incubated for 12 h and then fixed in PBS containing 4% paraformaldehyde. After being rinsed three times with PBS, cells were permeated with PBS containing 3% SDS for 3 min, and then stained with 500 ng/ml DAPI (Roche Diagnostics, Indianapolis, America) for 5 min at room temperature. Cells were then washed three times with PBS and visualized under a laser confocal microscopy. (TCS sp5, Leica) (DAPI ex = 358 nm, em = 461 nm). Apoptotic cells were determined by the characteristic nuclear fragmentation.

Early apoptosis of cells stained with Annexin V was assessed using an Annexin V-FITC Apoptosis Detection Kit (KeyGEN, Jiangsu, China) according to the manufacturer's instructions. MDA-MB-231 cells were cultured in DMEM culture medium supplemented with 10% FBS. The cells were seeded in a 6-well plate at 5×10^5 cells per well and incubated for 12 h at 37 °C under 5% CO_2 atmosphere to reattach. Freshly prepared solutions of L-BCPD-18MA were diluted with the medium. The medium was removed from the plate and 2 ml fresh medium containing PS at concentration of 0.5 and 1 μg/ml was added to the wells. Cells were incubated at 37 °C under 5% CO_2 atmosphere in dark for 24 h. The medium was removed and the cells were washed twice with PBS solution, and 2 ml fresh medium was added. The plate was illuminated for 200 s with laser of wavelength 678 nm at a power density of 50 mW/cm^2. Cells were continuously incubated for 4 h, detached using 0.25% (w/v) trypsin, washed twice with PBS containing 2.5% FBS, stained with the 50 μg/ml Annexin V-FITC conjugate in the presence of 10 μg/ml PI for 10 min at room temperature, and finally analyzed using a FACSCalibur flow cytometer (MACSQuant, Miltenyi Biotec, Germany).

4.3.7. Study of BCPD-18MA biodistribution

L-BCPD-18MA was injected intravenously into the tumor-bearing mice at a dose of 4 mg/kg body weight. At timed intervals, the mice were sacrificed. Biodistribution of L-BCPD-18MA was determined at 0.25, 1, 3 and 5 h post injection. Tissues from the heart, liver, spleen, lung, kidney, tumor and skin around the tumor were sampled for determination. All excised tissue samples were rinsed, weighed and homogenized with ice cold 0.9% (w/v) NaCl. Blood was obtained by eyeball removal. Heparin (156.25 U/ml) was added to prevent blood coagulation. The blood samples were centrifuged at 3000*g*/min for 5 min to obtain the plasma. And then 160 μl homogenate of each tissue except spleen, 100 μl homogenate of spleen and 100 μl plasma were separately transferred to a 2.0 ml reaction tube, followed by addition of 1.5 ml methanol/diethyl ether (1:4, v/v). The samples were immediately mixed for 3 min using a vortex mixer and then incubated under continuous shaking for at least 12 h. The organic phase was then separated by centrifugation at 16,000*g*/min for 5 min, evaporated to dryness under nitrogen and the solid residue was reconstituted in 200 μl of the mobile phase for subsequent HPLC analysis. HPLC analysis of BCPD-18MA was carried out using an Agilent 1100 System and G1314A Variable Wavelength Detector. HPLC (Agilent 1100, America) was equipped with a reverse phase C18 column (Agilent). The mobile phase was composed of methanol, tetrahydrofuran, water and acetic acid (57:32:10:1), and the flow rate was set at 1 ml/min. The column heater (Model 100, CBL photoelectron technology, Tianjin) was set at 30 °C. The eluent was monitored at 438 nm. The retention time for BCPD-18MA was about 4.25 min. The injection volume was 50 μl and the storage loop was 20 μl. The All samples were filtered through filtration membrane with 0.45 μm pores before analysis. The amount of BCPD-18MA in the tissue was expressed as ng/g wet weight. The measuring range was from 50 to 12,000 ng/g wet weight and the detection limit was 30 ng/g.

4.3.8. PDT study of BCPD-18MA in vivo

To evaluate the potential PDT efficacy of L-BCPD-18MA upon irradiation with the diode laser at 678 nm, the antitumor effect in LLC-bearing mice was investigated. To minimize interference from hair at the tumor surface, tumor regions were shaved with an animal shaver prior to light exposure. Experimental LLC-bearing mice were divided into seven groups according to different injections of treatment: (1) three negative control groups: (a) untreated, (b) light exposure only, (c) L-BCPD-18MA only at 2 mg/kg; (2) three PS test groups: (d) L-BCPD-18MA at 0.5 mg/kg plus light exposure, (e) L-BCPD-18MA at 2 mg/kg plus light exposure, (f) L-BCPD-18MA at 1 mg/kg plus light exposure; (3) positive control group: (g) L-BPDMA at 0.5 mg/kg plus light exposure. Each group contained 10 mice. Tumors were illuminated with laser light (300 mW/cm^2) for 500 s at 3 h after drug administration for a total light dose of 150 J/cm^2. The tumor size of the LLC-bearing mice was observed consecutively for 30 days.

Differences between groups with respect to the mean tumor volume were evaluated by using Student's *t*-test. The significance was accepted at $P < 0.05$. All statistical comparisons were done using the SPSS 10.0 for windows software.

4.3.9. Histopathology analysis

Five LLC-bearing mice were randomized into five groups as following: (a) control; (b) L-BCPD-18MA-treated at 5 mg/kg without light exposure; (c) L-BCPD-18MA-treated at 0.5 mg/kg and light exposure; (d) L-BCPD-18MA-treated at 1 mg/kg and light exposure; (e) L-BCPD-18MA-treated at 2 mg/kg and light exposure. The LLC-bearing mice from the latter three groups received illumination of light with a 678 nm wavelength laser at a dose of 150 J/cm^2 after drug administration. The mice were sacrificed by cervical dislocation at day 5 after treatment. The heart, liver, spleen, lung, kidney and tumors were excised, fixed in 10% formalin, paraffin embedded, sliced to 3 μm sections, and stained with haematoxylin and eosin (H&E) for microscopic analysis (DLMB, Leica).

Acknowledgments

This research was supported by the Nation Natural Science Foundation of China (Grant No. 30371737) and the National Science & Technology Major Project 'Major New Drug Creation Program' Foundation of China (Grant No. 2009ZXJ09003-028).

References and notes

1. Brown, S. B.; Brown, E. A.; Walker, I. *Lancet Oncol.* **2004**, *8*, 497.
2. Dougherty, T. J. *J. Clin. Laser Med. Surg.* **2002**, *1*, 3.
3. Ackroyd, R.; Kelty, C.; Brown, N.; Reed, M. *Photochem. Photobiol.* **2001**, *5*, 656.
4. Spikes, J. D. Porphyrin Localization and Treatment of Tumors and Other Diseases. In *Photobiology of Porphyrins*; Doiron, D. R., Gomer, C. J., Eds.; E-Publishing Inc.: New York, 1984.
5. Moan, J. *J. Photochem. Photobiol., B* **1990**, *6*, 343.
6. Detty, M. R.; Gibson, S. L.; Wagner, S. J. *J. Med. Chem.* **2004**, *16*, 3897.
7. Hayata, Y.; Konaka, C. Photodynamic Therapy of Neoplastic Disease. In *Photodynamic Therapy of Neoplastic Diseases*; Kessel, D., Ed.; CRC Press: Boca Raton, 1990.
8. Wening, B. L.; Kurttman, D. M.; Grossweiner, L. I.; Mafee, M. F.; Harris, D. M.; Lobraico, R. V.; Prycz, R. A.; Appelbaum, E. L. *Arch. Otolaryngol. Head Neck Surg.* **1990**, *11*, 1267.
9. McCaughan, J. S., Jr. *Cancer Invest.* **1990**, *3*, 407.
10. Buchanan, R. B.; Carruth, J. A.; McKenzie, A. L.; Williams, S. R. *Eur. J. Surg. Oncol.* **1989**, *5*, 400.
11. Sharman, W. M.; Allen, C. M.; van Lier, J. E. *Drug Discovery Today* **1999**, *4*, 507.
12. Dougherty, T. J.; Gomer, C. J.; Henderson, B. W.; Jori, G.; Kessel, D.; Korbelik, M.; Moan, J.; Peng, Q. *J. Natl. Cancer Inst.* **1998**, *90*, 889.
13. Boyle, R. W.; Dolphin, D. *Photochem. Photobiol.* **1996**, *3*, 469.
14. Svensson, J.; Johansson, A.; Gräfe, S.; Gitter, B.; Trebst, T.; Bendsoe, N.; Andersson-Engels, S.; Svanberg, K. *Photochem. Photobiol.* **2007**, *5*, 1211.
15. Richter, A. M.; Waterfield, E.; Jain, A. K.; Canaan, A. J.; Allison, B. A.; Levy, J. G. *Photochem. Photobiol.* **1993**, *6*, 1000.
16. Yao, J.; Zhang, W.; Sheng, C.; Miao, Z.; Yang, F.; Yu, J.; Zhang, L.; Song, Y.; Zhou, T.; Zhou, Y. *Bioorg. Med. Chem. Lett.* **2008**, *6*, 293.
17. Yao, J. Z.; Liu, J. F.; Zhang, W. N.; Zhou, Y. J.; Zhu, J.; Lü, J. G.; Wang, X. Y.; Li Chin, K. *J. Org. Chem.* **2001**, *21*, 458. in Chinese.
18. Kennedy, J. C.; Pottier, R. H. *J. Photochem. Photobiol., B* **1992**, *14*, 275.
19. Sadzuka, Y.; Iwasaki, F.; Sugiyama, I.; Horiuchi, K.; Hirano, T.; Ozawa, H.; Kanayama, N.; Oku, N. *Toxicol. Lett.* **2008**, *1*, 110.
20. Granville, D. J.; Hunt, D. W. *Curr. Opin. Drug Discov. Dev.* **2000**, *2*, 232.
21. Kessel, D.; Luo, Y. *J. Photochem. Photobiol., B* **1998**, *2*, 89.
22. Furre, I. E.; Møller, M. T.; Shahzidi, S.; Nesland, J. M.; Peng, Q. *Apoptosis* **2006**, *11*, 2031.
23. Wawrzyńska, M.; Kałas, W.; Biały, D.; Zioło, E.; Arkowski, J.; Mazurek, W.; Strzadała, L. *Arch. Immunol. Ther. Exp.* **2010**, *1*, 67.
24. Chiou, J. F.; Wang, Y. H.; Jou, M. J.; Liu, T. Z.; Shiau, C. Y. *Free Radical Res.* **2010**, *2*, 155.
25. Plaetzer, K.; Kiesslich, T.; Oberdanner, C. B.; Krammer, B. *Curr. Pharm. Des.* **2005**, *9*, 1151.
26. Saraste, A. *Herz* **1999**, *3*, 189.
27. Castano, A. P.; Demidova, T. N.; Hamblin, M. R. *Photodiagn. Photodyn. Ther.* **2005**, *2*, 91.
28. Richter, A. M.; Waterfield, E.; Jain, A. K.; Canaan, A. J.; Allison, B. A.; Levy, J. G. *Photochem. Photobiol.* **1993**, *57*, 1000.
29. Chen, B.; Pogue, B. W.; Hasan, T. *Expert Opin. Drug Deliv.* **2005**, *2*, 477.
30. Reddi, E. *J. Photochem. Photobiol., B* **1997**, *3*, 189.
31. Hoebeke, M. *J. Photochem. Photobiol., B* **1995**, *3*, 189.
32. Osterloh, J.; Vicente, M. G. *J. Porphyrins Phthalocyanines* **2002**, *5*, 305.
33. Derycke, A. S. L.; de Witte, P. A. M. *Adv. Drug Delivery Rev.* **2004**, *1*, 17.
34. Nyman, E. S.; Hynninen, P. H. *J. Photochem. Photobiol., B* **2004**, *1*, 1.
35. MacDonald, I. J.; Dougherty, T. J. *J. Porphyrins Phthalocyanines* **2001**, *2*, 105.
36. Bangham, A. D.; Standish, M. M.; Watkins, J. C. *J. Mol. Biol.* **1965**, *1*, 238.